

Preparation of Asymmetric Membranes and Their Applications in the Restoration of Groundwater Contaminated by Trichloroethylene via Two-Step Bioremediation Technology

Zhenyu Song,^{1,2,3} Wei Yang,^{1,2,3} Jinghui Zhang,^{1,3} Tao Bi,¹ Ye Li,^{1,2,3} Shanshan Yuan^{1,3}

¹Tianjin Eco-City Environmental Protection Limited Company, Tianjin 300467, People's Republic of China

²Sino-Singapore Tianjin Eco-City Postdoctoral Programme, Tianjin 300467, People's Republic of China

³Tianjin Contaminated Site Remediation Technology Engineering Center, Tianjin 300467, People's Republic of China

Correspondence to: W. Yang (E-mail: yangwei@tjeco-city.com)

ABSTRACT: Asymmetric hollow-fiber membranes were fabricated via a thermally induced phase-separation process, and the properties of the membrane were investigated. A bubbleless-aeration membrane module (BAMM) was designed for the purpose of releasing hydrogen or oxygen. Then, the anaerobic reductive dechlorination (ARD) remediation zone and the aerobic oxidative decomposition (AOD) remediation zone were founded based on the BAMM. The effects of the aeration pressure of hydrogen and oxygen on the oxidation reduction potential (ORP) of the liquid phase were investigated. The groundwater contaminated by trichloroethylene (TCE) was used as the restoring object. The effect of the hydrogen aeration on the ARD process and the effect of the oxygen aeration on the AOD process were also investigated. The results show that the ORP-retention time curve in the ARD zone presented an upward opening parabola of growth, whereas the ORP-retention time curve in the AOD zone presented a downward opening parabola of growth. It took 8 days for TCE to decrease from 500 to 52 $\mu\text{g/L}$ in the ARD zone, whereas it took 24 h for *cis*-dichloroethylene to decrease from 52 to 35 $\mu\text{g/L}$ in the AOD zone. © 2014 Wiley Periodicals, Inc. *J. Appl. Polym. Sci.* **2014**, *131*, 41176.

KEYWORDS: bioengineering; fibers; membranes

Received 12 February 2014; accepted 13 June 2014

DOI: 10.1002/app.41176

INTRODUCTION

Chlorohydrocarbons, represented by trichloroethylene (TCE),^{1–3} have been widely used in metal processing, dry cleaning, electroplating, organic synthesis, and so on. The leakage and improper discharge of chlorohydrocarbons has caused serious groundwater contamination. TCE is toxic, causing carcinogenesis, teratogenesis, and mutagenesis. *cis*-Dichloroethylene (*cis*-DCE),^{4,5} which is the degradation product of TCE, is still a cancerogenic substance.

TCE belongs to dense nonaqueous phase liquids (DNAPLs).^{6–10} DNAPLs are minimally soluble in water, more dense than water, and present in concentrations large enough to form pools of free liquid. DNAPLs tend to sink and accumulate on a non-permeable layer at the bottom of a confined aquifer and become a persistent pollution source. The control and cleanup of TCE contamination in the groundwater is a research hotspot in the remediation of contaminated sites.

The traditional pumping and treatment technique usually fails to restore TCE contamination because of DNAPLs absorbed on soil particles.¹¹ The chemical oxidation¹² method can decompose TCE in the source zone, but this would present the risk of

the site becoming alkaline. The chemical reduction¹³ method with zero-valent iron as the reductant was efficient for degrading TCE to less chlorinated compounds. However, surface oxidation results in the invalidation of zero-valent iron.

Innovative technologies, especially bioremediation,^{14,15} have been developed and implemented in an effort to reduce the cost and time required to clean up TCE contamination. In comparison to other technologies, bioremediation is usually less expensive, does not require waste extraction or excavation,¹⁶ and is more publicly acceptable as it relies on natural processes to treat contamination.

Bioremediation uses microorganisms to degrade organic contaminants in soil, groundwater, sludge, and solids either excavated or *in situ*. Microorganisms break down contaminants with them as a food source or by cometabolization with a food source. Aerobic processes require an oxygen source, and the end products typically are carbon dioxide and water. Anaerobic processes are conducted in the absence of oxygen, and the end products can include methane, sulfide, elemental sulfur, and dinitrogen gas.

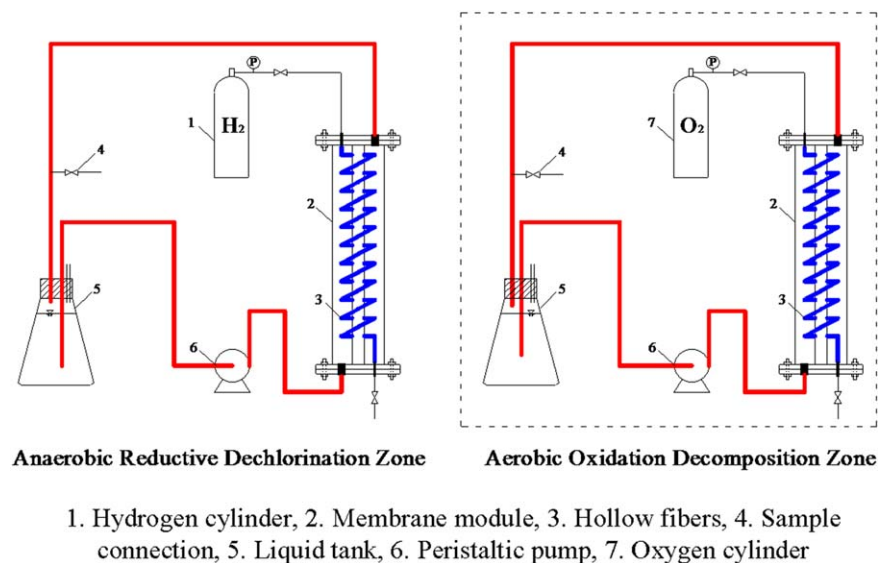


Figure 1. Schematic of the bubbleless-aeration restoring groundwater experiment. [Color figure can be viewed in the online issue, which is available at wileyonlinelibrary.com.]

However, in the anaerobic reductive dechlorination (ARD) process of restoring TCE, the lack of hydrogen in natural conditions results in the half reduction of TCE contamination.^{17,18} In addition, *cis*-DCE, the primary reduction product of TCE, has a very slow reduction rate.

In this article, a novel bubbleless-aeration device used for releasing remediation gas was developed. The asymmetric hollow-fiber membranes were prepared via a thermally induced phase-separation process. The asymmetric membrane was used as a carrier for supplying hydrogen or oxygen to the biofilm. Through the asymmetric membrane, the dechlorinating bacteria acquired the electron donor (hydrogen) used for restoring TCE, and the oxidizing bacteria acquired the electron acceptor (oxygen) used for decomposing *cis*-DCE. Finally, a two-step bioremediation technology, including the ARD process and aerobic oxidative decomposition (AOD) process, was established.

EXPERIMENTAL

Preparation of the Hollow-Fiber Membranes

Materials. Isotactic polypropylene (iPP; average molecular weight = 412,000) was purchased from Daqing Petroleum Chemical (People's Republic of China). Dioctyl phthalate (DOP), dibutyl phthalate (DBP), and ethanol were analytical reagents and were purchased from Guangfu Fine Chemical Research Institute (People's Republic of China). All chemicals used in this study were not purified further.

Hollow-Fiber Membrane Preparation. Hollow-fiber membranes were fabricated by an extrusion apparatus. Measured amounts of iPP and mixed diluent were stirred in the vessel heated to 180°C for 6 h under a nitrogen atmosphere. After it was kept at 180°C for 2 h to remove the bubbles, the homogeneous iPP solution was fed into a spinneret under a nitrogen pressure of 0.2 MPa. The nitrogen was used as a bore fluid to make a lumen of the hollow fiber. The hollow fiber was extruded from the spinneret and wound on a take-up winder

after it was placed in a water bath at 25°C to induce the phase separation and solidify the membrane. The air gap between the spinneret and the water bath was 20 cm. The residual mixed diluent in the hollow fiber was extracted by immersion in ethanol for 24 h, and then, ethanol was removed by the immersion of the membrane into water. At last, the wetted fibers were dried in air at room temperature.

Characterization of the Hollow-Fiber Membranes. The morphologies of the hollow fibers were observed with a Philips XL30 scanning electron microscope.

The tensile strength and breaking elongation of a single hollow fiber were measured by a WD-10D instrument (Changchun Second Testing Machines, People's Republic of China). The gauge length and X-head speed were 40 mm and 50 mm/min, respectively.

The gas permeance of the hollow fiber was measured by the linking of the fibers to an air compressor and a soap film flow meter, which had a pressure-regulating valve and a pressure gauge. The air was forced to permeate from the inside to the outside of the fiber under a pressure of 0.1 MPa. The gas permeance was calculated on the basis of the inner surface area of the hollow fiber.

Restoration of Contaminated Groundwater via Membrane Aeration

Membrane Aeration Experiment. A wind-type membrane module was prepared for membrane aeration. The aeration membrane module was made by 30 hollow fibers with a length of 2500 mm. The fibers were twisted on a solid cylinder with a diameter of 500 mm and filled into a cylindrical shell. The membrane area of the module was 0.142 m².

The schematic diagram of restoring contaminated groundwater via membrane aeration is shown in Figure 1. Two zones were founded with two membrane modules and distinguished by aeration with hydrogen and oxygen. In the ARD zone, the aqueous

Table I. Compositions of the Inorganic Salt Nutrient Solution

Substance	Concentration (mg/L)	Substance	Concentration (mg/L)
NH ₄ Cl	320	(NH ₂) ₂ CS	667
KH ₂ PO ₄	63	Na ₂ CO ₃	132
CaCl ₂	63		

solution was circulated by a peristaltic pump. Hydrogen permeated through the membrane under the driving force of pressure and dissolved in the liquid phase. Hydrogen was used by dechlorinating bacteria as an electron donor. In AOD zone, the hydrogen was replaced by oxygen. The aqueous circulation was carried out by a peristaltic pump. The revolving speed of the two pumps remained at 130 rpm throughout the whole aeration process. The volume of the aqueous solution was 500 mL.

Biofilm Formation and Domestication. The anaerobic activated sludge (AS) inoculated into the ARD zone was derived from an anaerobic tank from the Sino-Singapore Eco-City Yingcheng sewage treatment plant. After the anaerobic AS circulated in the membrane module for 8 h, most of the AS was captured and adsorbed on the hollow fibers. Then, 500 mL of an inorganic salt nutrient solution and 10 mL of a microelement nutrient solution were added to the feed flask. The mass ratio of the nutrient elements of carbon, nitrogen, and phosphorus reached 200:5:1. The domestication of the microorganism was carried out with the nutrient-solution-dissolved TCE. In the domestication process, the TCE concentration was maintained at 400–500 $\mu\text{g/L}$, the hydrogen aeration pressure was controlled at 0.25 MPa, the circulation velocity of the solution was 50 mL/min, and the domestication time was 30 days. The compositions of the inorganic salt nutrient solution and microelement nutrient solution are shown in Tables I and II, respectively.

The aerobic AS inoculated into the AOD zone was derived from the secondary sedimentation tank from the Sino-Singapore Eco-City Yingcheng sewage treatment plant. The biofilm formation time and composition of nutrient solution were same as those in the ARD zone. The domestication of the microorganism was carried with the nutrient-solution-dissolved TCE and *cis*-DCE. Both the concentrations of TCE and *cis*-DCE were maintained at 200–300 $\mu\text{g/L}$. The oxygen aeration pressure was 1.0 MPa, and the domestication time was 30 days.

Table II. Compositions of the Microelement Nutrient Solution

Substance	Concentration (mg/L)	Substance	Concentration (mg/L)
MgSO ₄ ·7H ₂ O	500	CuSO ₄ ·5H ₂ O	5
FeCl ₂ ·4H ₂ O	600	NiSO ₄ ·6H ₂ O	88
CoCl ₂ ·6H ₂ O	104	MnCl ₂ ·4H ₂ O	500
H ₃ BO ₃	10	(NH ₄) ₆ Mo ₇ O ₂₄ ·4H ₂ O	64

Table III. Groundwater Properties

Detection index	Concentration (mg/L)	Detection index	Concentration (mg/L)
Permanganate index	9.62	Mercury	0.00001
Ammonia nitrogen	0.294	Copper	0.001
Total hardness	3874	Arsenic	0.005
Chloride	10,940	Cadmium	0.001
Nitrate	17.1		

The data of the groundwater conditions were provided by Tianjin Eco-City Environmental Testing Center Co., Ltd.

The nutrient solution in the experiment was prepared with the groundwater from Sino-Singapore Eco-City Duishan Park. The groundwater conditions are shown in Table III.

Analysis. The concentrations of TCE and *cis*-DCE were determined with gas chromatography on an HP-1 column. The temperature program was 50°C for 2 min, with ramping at 25°C/min to 200°C. The helium gas flow rate was 30 mL/. The injector and detector temperatures were 160 and 300°C, respectively. The peaks were identified by coelution with known standards, and the detector responses were calibrated as the relative responses of the analysis to the internal standard on a multilevel standard curve. The limits of detection were 0.2 $\mu\text{g/L}$.

The oxidation reduction potential (ORP) was detected by pH340i (WTW Corp., Germany).

RESULTS AND DISCUSSION

Hollow-Fiber Membrane Characterization

The hollow-fiber membranes were prepared via a thermally induced phase-separation process. The iPP concentration in the casting membrane solution was 40 wt %, and the DBP concentrations in the mixed diluent were 40 and 80 wt %, respectively. Therefore, two types of hollow-fiber membrane (fibers 1 and 2) were prepared.

The micromorphologies of fibers 1 and 2 are shown in Figures 2 and 3, respectively. The cross section of fiber 1 presents a fuzzy spherulitic structure. The pores in the fuzzy spheres disconnected with each other. The cross section of fiber 2 showed a bicontinuous structure with a good connectivity because a weak compatibility existed between iPP and the mixed diluent. Both the outer surfaces of the two hollow fibers possessed a dense skin. This was due to the evaporation of mixed diluent when the hollow fiber passed through the air gap between the spinneret and coagulant bath. As the DBP concentration in mixed diluent increased from 40 to 80 wt %, the average pore size of the inner surface increased from 2.52 to 3.64 μm .

As influenced by the membrane morphology, fiber 2 had a larger gas performance and a better tensile strength than fiber 1, as shown in Table IV. Fiber 2 seemed more suitable for use as a bubbleless-aeration membrane, which is applied in contaminated groundwater bioremediation. Therefore, fiber 2 was used in a two-step bioremediation experiment, and the impact of the operating factors on the bioremediation efficiency was tested.

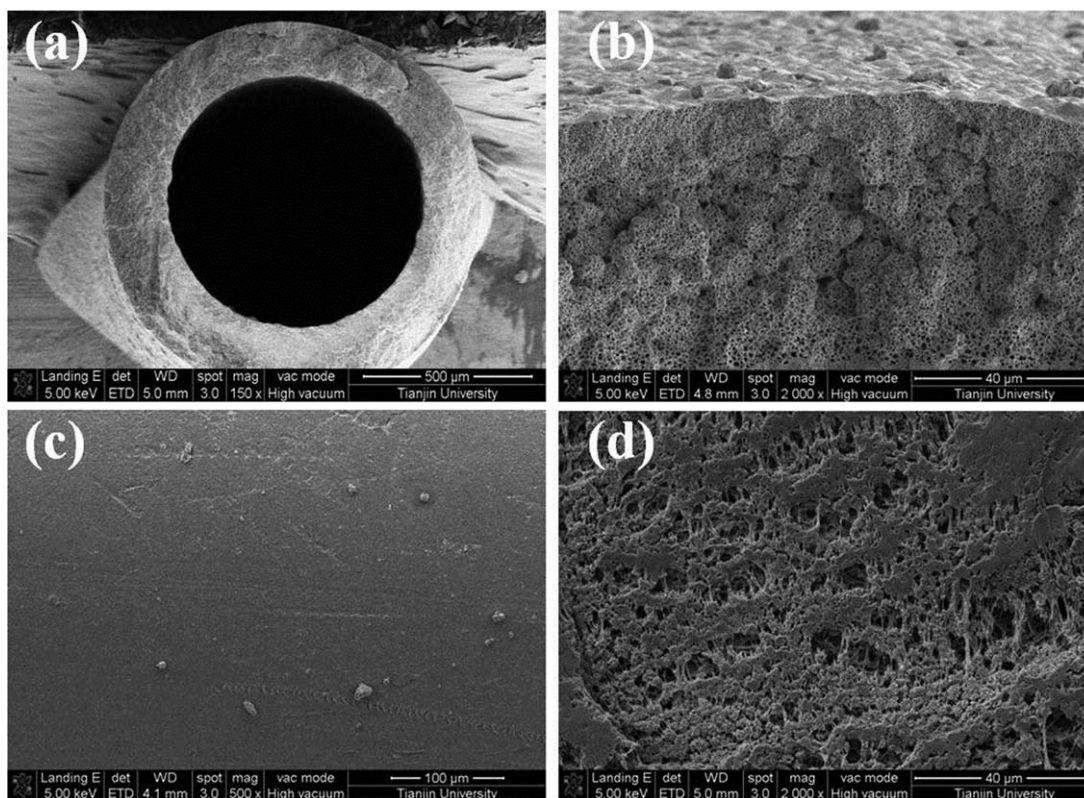


Figure 2. Scanning electron microscopy photograph of fiber 1: (a) overview, (b) cross section, (c) outer surface, and (d) inner surface.

Impact of the Aeration Pressure on ORP

We determined the ARD zone by providing the aqueous phase with hydrogen via a bubbleless-aeration membrane module (BAMM). Meanwhile, we determined the AOD zone by providing the aqueous phase with oxygen via the BAMM. ORP was investigated as an experimental object for the purpose of investigating the efficiency of the bubbleless aeration. The impacts of the aeration pressures of hydrogen and oxygen were examined in the absence of the AS, respectively.

Figure 4 shows the impact of the hydrogen aeration pressure on ORP. The ORP decreased with increasing residence time at each hydrogen aeration pressure. The driving force of hydrogen transmission into the aqueous phase was the difference between the vapor-phase pressure and equilibrium partial pressure of the aqueous phase. The driving force of hydrogen transfer decreases with increasing dissolved hydrogen concentration in the aqueous phase. Therefore, the ORP–residence time curves presented an upward-facing opening parabola of the growth characteristics.

As shown in Figure 4, the ORPs approached equilibrium values at each hydrogen aeration pressure with the residence time of 18 h. The equilibrium value decreased with increasing hydrogen aeration pressure. This was due to the increase of the driving force of the hydrogen transfer, which was caused by the increasing vapor-phase pressure at the surface of the membrane. The ORP of the aqueous phase achieved a value of -534 mV at the hydrogen aeration pressure of 1.0 MPa and the residence time of 24 h.

Under the conditions of the absence of AS, the impact of the oxygen aeration pressure on ORP is shown in Figure 5. The ORP value was enhanced as the residence time increased at each oxygen aeration pressure. The ORP–residence time curves presented a downward opening parabola of growth. This was also caused by the variation of the driving force of oxygen transfer. The ORPs approached equilibrium values at each oxygen aeration pressure with a residence time of 15 h. The ORP of the aqueous phase achieves a value of 451 mV at an oxygen aeration pressure of 1.0 MPa and a residence time of 24 h.

Although the increase in the aeration pressure was beneficial for enhancing the transfer driving force of the remediation gas, a mass of large bubbles emerged from the surface of the hollow-fiber membrane when the aeration pressure was higher than 1.2 MPa. The large bubbles decreased the utilization rate of remediation gas. In addition, this also caused the biofilm to strip away the hollow-fiber membrane; this was harmful for the microorganism capture of the remediation gas. Therefore, the maximum aeration pressure was set at 1.0 MPa in the bioremediation experiment.

Impact of Hydrogen Aeration on the ARD Process

A TCE solution with a concentration of $500 \mu\text{g/L}$ was prepared with groundwater from Sino-Singapore Duishan Park. The hydrogen aeration pressure was fixed at 1.0 MPa in the ARD zone. The hydrogen that was used by the dechlorinating bacteria as an electron donor played an important role in the ARD process, whereas TCE performed as an electron acceptor. As shown

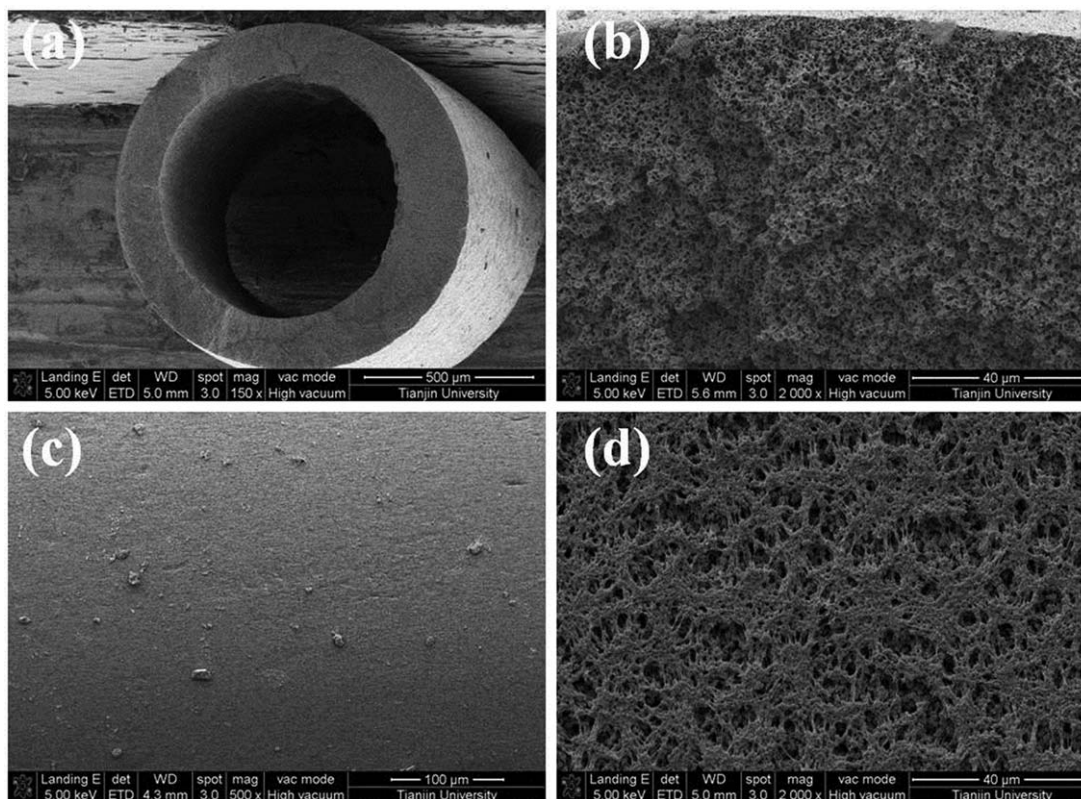


Figure 3. Scanning electron microscopy photograph of fiber 2: (a) overview, (b) cross section, (c) outer surface, and (d) inner surface.

in Figure 6, as the residence time increased, both the TCE consumed by the dechlorinating bacteria and the *cis*-DCE restored from TCE increased gradually. Within the scope of the experimental time, the reducing function of the dechlorinating bacteria acting on *cis*-DCE was very limited. This could be explained by the variation of the driving force of the redox reaction. The ORP of *cis*-DCE was 490 mV lower than that of TCE.^{19,20} The capacity of the dechlorinating bacteria to restore *cis*-DCE was reduced significantly compared with the capacity to restore TCE, especially with the existence of TCE.

As shown in Figure 6, as the residence time through the ARD zone was 8 days, the TCE concentration in aqueous phase decreased from 500 to 52 $\mu\text{g/L}$, and the *cis*-DCE concentration increased from 0 to 219 $\mu\text{g/L}$. It should be noted that the screening level of TCE was 70 $\mu\text{g/L}$ in “Guidelines for Risk Assessment of Contaminated Sites” (Exposure Draft) of China.

Table IV. Properties of the Hollow-Fiber Membranes

Property	Fiber 1	Fiber 2
Inner diameter (μm)	425	410
Thickness (μm)	120	110
Gas permeance (GPU)	2892	7895
Tensile strength (MPa)	1.125	2.448

1 GPU = $1 \times 10^{-6} \text{ cm}^3(\text{STP}) \text{ cm}^{-2} \cdot \text{s}^{-1} \cdot \text{cmHg}^{-1}$.

This screening level was achieved at the residence time of 5 days in the experiment.

Impact of Oxygen Aeration on the AOD Process

The remediation object of the AOD zone was aimed at the product of the ARD zone. The outlet water with a residence time of 8 days from the ARD zone was used as an experimental subject. The oxygen aeration pressure of the AOD zone was fixed at 1.0 MPa. The impact of the oxygen aeration on the AOD process is shown in Figure 7. As the residence time of the

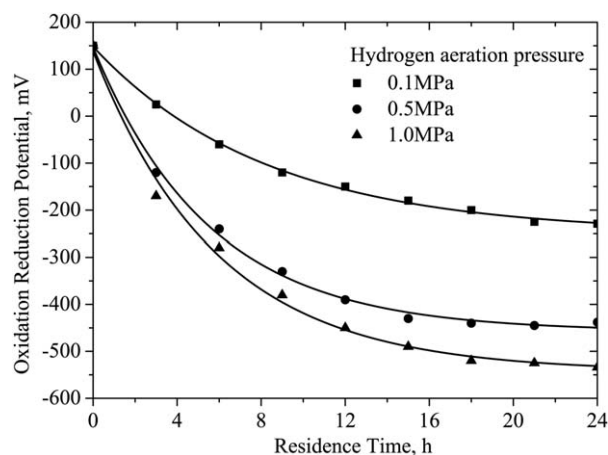


Figure 4. Impact of the hydrogen aeration pressure and residence time on ORP.

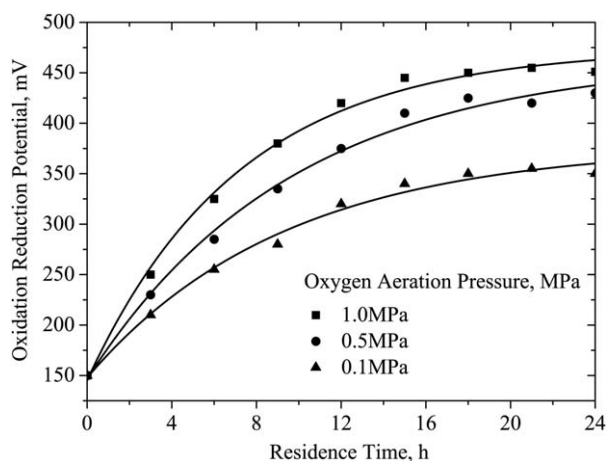


Figure 5. Impact of the oxygen aeration pressure and residence time on ORP.

aqueous phase increased, the *cis*-DCE concentration dropped rapidly; however, the TCE concentration only presented a slight downward trend. The ORP of the *cis*-DCE was relatively low and presented obvious reducibility. The *cis*-DCE, which was used by aerobic bacteria as an electron donor, was oxidized into carbon dioxide, water, and chlorine. The oxygen serving as an electron acceptor was restored into water. The ORP of TCE was relatively high, in that TCE had a weak reducibility. The degradation function of the aerobic bacteria for TCE was quite limited in a short time. With the residence time of 48 h, the *cis*-DCE concentration decreased from 219 to 32 $\mu\text{g/L}$, whereas the TCE concentration only decreased from 52 to 35 $\mu\text{g/L}$. The "Guidelines for Risk Assessment of Contaminated Sites" (Exposure Draft) of China stipulates the screening level of *cis*-DCE as 50 $\mu\text{g/L}$. As shown in Figure 7, the *cis*-DCE concentration achieved this screening level with a residence time of 30 h.

CONCLUSIONS

Asymmetric hollow-fiber membranes were prepared via a thermally induced phase-separation process. With the BAMM as the

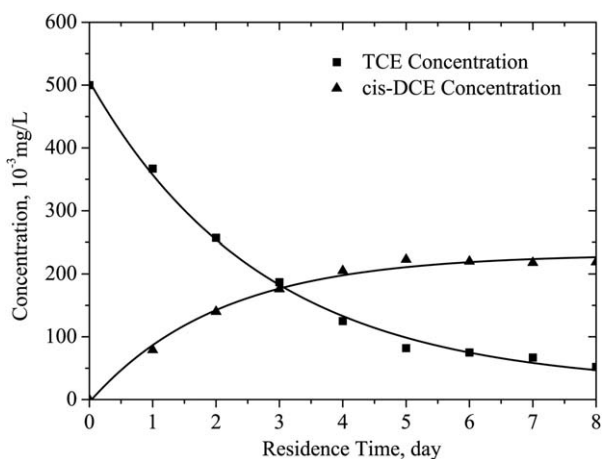


Figure 6. Variation of the TCE and *cis*-DCE concentrations with the residence time in the ARD area.

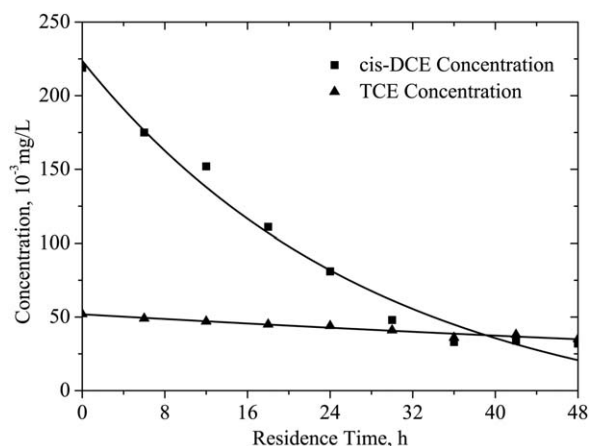


Figure 7. Variation of the TCE and *cis*-DCE concentrations with the residence time in the AOD area.

releasing device of hydrogen and oxygen, the anaerobic reductive remediation zone and the AOD remediation zone were founded on the basis of the module. After the experiments on restoring the groundwater contaminated by TCE, some conclusions were made as follows:

1. The results show that the ORP–retention time curve in the anaerobic reductive remediation zone presented an upward opening parabola of growth.
2. The ORP–retention time curve in the AOD remediation zone presented a downward opening parabola of growth.
3. It took 8 days for TCE to decrease from 500 to 52 $\mu\text{g/L}$ in the ARD zone, although it took 24 h for *cis*-DCE to decrease from 52 to 35 $\mu\text{g/L}$ in the AOD zone.

REFERENCES

1. Yusaku, M.; Akiyoshi, S.; Hiroaki, Y.; Hirota, K.; Motoyuki, S. *Water Res.* **2003**, *37*, 1852.
2. Gregory, A. L. *Water Res.* **2001**, *35*, 1453.
3. Cheng, S.; Wu, S. *Chemosphere* **2001**, *43*, 1023.
4. Steven, W. C.; Beth, L. P.; John, A. C. *J. Contaminant Hydrology* **2007**, *91*, 203.
5. Zuhail, O.; Berrin, T.; Yelena, K.; Michael, S.; Shonali, L. *Chemosphere* **2012**, *89*, 665.
6. Muhammad, F.; Iftikhar, A. R.; Arshad, P. *Solar Energy* **2009**, *83*, 1527.
7. Haest, P. J.; Springael, D.; Seuntjens, P.; Smolders, E. *Chemosphere* **2012**, *89*, 1369.
8. Mark, H.; Angela, F. *J. Contaminant Hydrology* **2013**, *151*, 16.
9. Beth, L. P.; John, A. C.; Steven, W. C. *J. Contaminant Hydrology* **2004**, *74*, 197.
10. Chanat, C.; Steve, C.; Chainarong, S.; Bruce, D. *J. Hazard Mater.* **2014**, *268*, 177.
11. Chang, L. C.; Chu, H. J.; Hsiao, C. T. *J. Hydrology* **2007**, *342*, 295.
12. Thomas, H. C.; Poul, L. B.; Steven, A. B.; Rasmus, J.; Gorm, H.; Albrechtsen, H. *J. Contaminant Hydrology* **2000**, *45*, 165.

13. Fu, F.; Dionysios, D. D.; Liu, H. *J. Hazard Mater.* **2014**, *267*, 194.
14. Fatihah, S.; Fazli, R.; Mohd, R. T.; Nuraini, H.; Razali, M. R.; Alia, K.; Ainon, H. *Int. Biodeterioration Biodegrad.* **2014**, *90*, 115.
15. Elsa, L.; Alessandro, B.; Christof, H.; Barry, D. A. *J. Contaminant Hydrology* **2014**, *160*, 21.
16. Yang, H. Q.; Zeng, Y. Y.; Lan, Y. F.; Zhou, X. P. *Int. J. Rock Mech. Mining Sci.* **2014**, *69*, 59.
17. Haest, P. J.; Springael, D.; Smolders, E. *Water Res.* **2010**, *44*, 331.
18. Anne, K. F.; Axel, C. H.; Rasmus, J.; Albrechtsen, H.; Evan, C.; Poul, L. B. *Water Res.* **2007**, *41*, 355.
19. Vogel, T. M.; McCarty, P. L. *J. Contaminant Hydrology* **1987**, *1*, 299.
20. Vogel, T. M.; Criddle, C. S.; McCarty, P. L. *Environ. Sci. Technol.* **1987**, *22*, 722.